Buckling Behaviour of Clamped-Clamped Rectangular Thin Plates Composite Materials for a Zig-Zag Model

Hussam Hussein Ali **Majid Habeeb Faidh-Allah**

Mechanical Department, College of Engineering, University of Baghdad, Baghdad, Iraq

E-mail: ha391799@gmail.com E-mail: dr_majidhabeeb@yahoo.com

Submission date:- 20/5/2018	Acceptance date:-5/6/2018	Publication date:-2/9/2018

Abstract

This paper focused mainly on the behavior buckling for the rectangular laminated plates made from three types of composite materials of a zig-zag model such as E-glass fiber / polyester (GFRP), carbon fiber / polyester (CFRP) and hybrid fibers / polyester (HFRP), under static buckling load and at room temperature (25C°). All the effects of plate determinants on the buckling load were studied for one type of a boundary condition, which was fixed on both sides, is clamped-clamped and free-free in other sides. The buckling analysis of these plates has been studied numerically and experimentally with different aspect ratio and constant thickness ratio. The experimental part is including the manufacture of composite materials laminated plates of a zig-zag model and determine the mechanical properties such as modulus of elasticity, yield stress, ultimate tensile strength and Poisson's ratio by tensile test for three types of composite materials such as GFRP, CFRP, and HFRP. The experiments of shear stress test was used to determine whether the layers would be the plates is delaminate layers during buckling test or not into the three types of composite materials samples. Experiments were also used to find the critical buckling load and maximum buckling deflection for clamped-clamped rectangular laminated plates of three types of composite materials for a zig-zag model with the effect of aspect ratios under uniformly distributed static compression load.

Numerical analysis of critical buckling load and maximum buckling deflection are calculated for three types of composite materials thin plates for a zig-zag model with the effect of aspect ratios under uniformly distributed static buckling load, the finite elements method was used in ANSYS program version (15.0).

The main conclusion of this research is that the presence of zig-zag fibers in the plate can improve the mechanical properties and increase the critical buckling load. The maximum percentage errors between the experimental and numerical results are 29.23%, 30.20%, and 46.71% at aspect ratio (a/b=1) for GFRP, CFRP, and HFRP, respectively. The maximum deflection value is increased when the aspect ratio is increased under constant thickness ratio; also, the maximum deflection in GFRP composite materials rectangular laminated plates is greater than that in CFRP and HFRP.

A good agreement is achieved between the two experimental ways for determining the critical buckling load and maximum buckling deflection results, the maximum absolute percentage error rates are about 1% and 1.1%, respectively.

Key words: Buckling Analysis, Zig-zag composite materials, Clamped-clamped plates, ANSYS R15.

Nomenclature

Symbol	Description	Units
E	Modulus of elasticity	GN/m^2
h	Plate thickness	mm
a	Plate length	mm
b	Plate width	mm
P_{cr}	Critical buckling load	kN
t	Time	sec
ρ	Material density	kg/m^3
τ	Shear stress	MN/m^2
ϑ	Poisson's ratio	/
σ_{buck}	Ultimate buckling stress	MN/m^2

1. Introduction

The failure designing failures structures are with many sorts, some of them incorporate creep, fatigue, substitute stresses, bending, buckling and so on. buckling happens in segments, plates, shells, and different structures of standard or unpredictable geometry **[11]**

In case that the loads connected to a level plate are low then there is low no watched mutilation of the plate however as the load is expanded then the harmonious arrangement of the plate changes into no level setup. Along these lines the plate for the situation complete noticeably insecurity.

The critical buckling load was called for the balance is bothered at which the minimum load, laminated composite plates are getting to be in auxiliary applications and in an extensive assortment of structures including aviation, marine and common framework progressively utilized owing in light of their high particular strength (failure stretch/unit weight) and particular stiffness (stiffness/unit weight).

Many focal points they offer:(high quality/solidness) for lower weight, amazing exhaustion reaction, qualities, aperients to alter fiber directions, substance and accumulating type, impedance to electrochemical consumption, and other fantastic material properties of composites.

example, the three- Along with this, various laminate theories have been developed, for dimensional theories, smeared plate theories, layer-wise models,zigzag models, and global-local models.**[1]**

Lee et al [1], considered the laminate bending of composite materials plates for a zigzag model It is likely that the rest contrasts between the outcomes from correct flexibility examination and the present enhanced zig-zag model particurally in the mid-plane district are expected to the nonattendance of thickness disfiguring. **Austin [2]**, examined the composite laminated plates with fiber reinforced polymer (FRP) for arrangement angles (90^o / $+45^o$ / -45^o) and showed the buckling loads at critical for overlays simply-supported on all edges, and for the anther boundary conditions, simply / simply / simply / free and simply / fixed / simply / free, where it shows up the better option is (90^o / $+15^o$ / -15^o) for aspect proportion under two value It has too been displayes that the proximity of curve bend -twist lessens the load of buckling fora cover plate up to 30%. **Esfahani [3]**, assessed exploratory and numerical buckling examination of delaminated hybrid composite beam structures it is detectable that this sort of replicating is sensible for direct buckling behavior of composite beam. regardless, in the examination are not considered post buckling and delamination crush. **Ahmed [4]**, concluded experimental and numerical realization of thermal and mechanical Loads of Buckling of Composite Laminated Plates it can be take out that the uniaxial buckling load increments with high rate when the quantity of stiffeners expanded, in SSSS, SFSF,.

Gaira et al [5], studied linear buckling analysis of laminated composite plate. **Al Humdany [6]**, discussed **t**heoretical and numerical analysis for buckling of anti-symmetric of simply supported laminated plates under uniaxial loads The buckling load depends essentially on the modulus ratio E1 /E2, largest values of the buckling load take place in the domain of angle of ply direction of the laminate between 30o-60o for each size and The maximum value occurs at α=45o for each size. **Joshi et al [7]**, analyzed the composite materials for thin carbon/epoxy plate with annular cut-outs under biaxial compression by using FEA It was noticed that the buckling load/unit length diminish with increments of perspective ratio. As the b/t proportion raises the buckling load decrease. **Ealavarasan** and **Selvarasu [8]**, investigated and analyzed the woven glass epoxy laminated composite Plate under buckling loads experimentally. The buckling load diminishes as the a/t proportion increments. The rate of reduction of buckling loads is not regular with the rate of increment of a/t ratio. **Rajappan et al [9]**, analyzed in unidirectional glass epoxy laminated plate under buckling loads from those results, the displacement is higher for rectangular notched plate than the others like plain and circular notched plates.

2. Theoretical Part

2.1 Basic assumptions

Fundamental presumptions for thin plates were given by Kirchhoff for the classical linear thin plate hypothesis (CPT) and by von Karman and Marquerre for the nonlinear CPT. They made their suppositions for isotropic materials. Various authors have expanded those suspicions for orthotropic or even for composite multilayer thin plates **[10], [11]**. The suppositions are as per the following:

- The plate is homogeneous (for instance, isotropic homogenization is made for a fiber composite-resin matrix and fiber-reinforced).
- The plate is thin—other dimensions (length and width) are no less than 10 times higher than the plate thickness.
- The material of the plate is deformable and it is subjected to Hooke's law;
- The plane stress state is considered for the plate—the stress acting in the plate plane rules the plate conduct, stresses acting toward the path typical to the plate plane are thought to be zero;
- All strains (ordinary and shear) in the plate plane are low compared with Because of these presumptions, the displacements can be depicted completely regarding the deformation of the mid-surface plane; consequently, the plate is diminished to the investigation of a two-dimensional issue comprising of the plate mid-surface. **Figure (1)** displays the u and v displacement suppositions in the x-z and y-z planes separately. **[11]**

$$u(x.y)=u_o(x.y)-z\frac{\partial w_0}{\partial x} \quad (1a)$$

$$v(x.y)=v_o(x.y)-z\frac{\partial w_0}{\partial y} \quad (1b)$$

$$w(x.y)=w_o(x.y) \quad (1c)$$

Where $\frac{\partial w_0}{\partial x}, \frac{\partial w_0}{\partial y}$ denote the rotations about y and x-axis respectively.

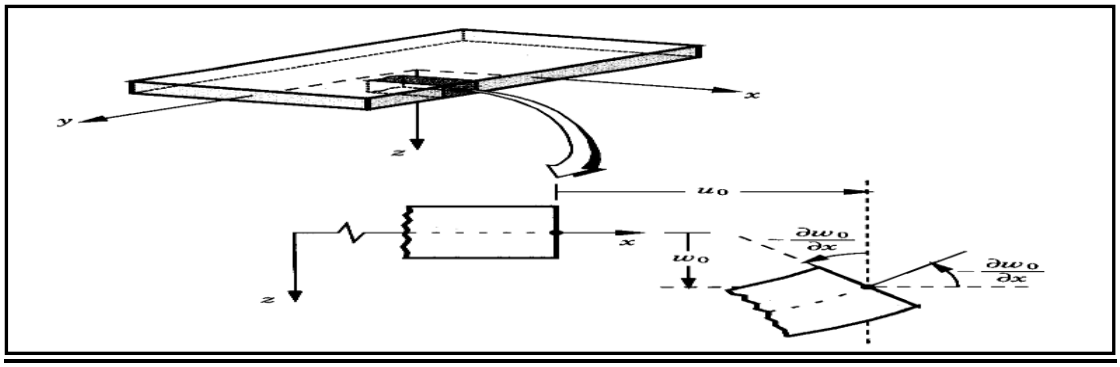

Fig.1: Deformed and undeformed geometries of an edge of a plate under the Kirchhoff assumptions. [11]

2.2 Stress and strain

The strain-displacement matrix relations take the form: **[11] [12]**

$$\begin{Bmatrix}\varepsilon_{xx}\\ \varepsilon_{yy}\\ \gamma_{xy}\end{Bmatrix}=\begin{Bmatrix}\varepsilon_{xx}^{(0)}\\ \varepsilon_{yy}^{(0)}\\ \gamma_{xy}^{(0)}\end{Bmatrix}+z*\begin{Bmatrix}\varepsilon_{xx}^{(1)}\\ \varepsilon_{yy}^{(1)}\\ \gamma_{xy}^{(1)}\end{Bmatrix}=\begin{Bmatrix}\frac{\partial u_o}{\partial x}\\ \frac{\partial v_o}{\partial y}\\ \frac{\partial u_o}{\partial y}+\frac{\partial v_o}{\partial x}\end{Bmatrix}+z*\begin{Bmatrix}-\frac{\partial^2 w_o}{\partial x^2}\\ -\frac{\partial^2 w_o}{\partial y^2}\\ -2\frac{\partial^2 w_o}{\partial x\,\partial y}\end{Bmatrix} \quad (2)$$

The membrane strains which are $(\varepsilon_{xx}^{(0)}.\varepsilon_{yy}^{(0)}.\gamma_{xy}^{(0)})$ and the flexural (bending) strains are $(\varepsilon_{xx}^{(1)}.\varepsilon_{yy}^{(1)}.\gamma_{xy}^{(1)})$, known as the curvatures **[12]**.

The transformed stress-strain relations of an orthotropic lamina in a plane state of stress are; for$\bar{Q}_{ij}$:

$$\begin{Bmatrix}\sigma_{xx}\\ \sigma_{yy}\\ \sigma_{xy}\end{Bmatrix}_k = \begin{bmatrix}\bar{Q}_{11} & \bar{Q}_{12} & \bar{Q}_{16}\\ \bar{Q}_{12} & \bar{Q}_{22} & \bar{Q}_{26}\\ \bar{Q}_{16} & \bar{Q}_{26} & \bar{Q}_{66}\end{bmatrix}_k \begin{Bmatrix}\varepsilon_{xx}\\ \varepsilon_{yy}\\ \gamma_{xy}\end{Bmatrix} \quad (3)$$

The resultant of in-lane force N_{xx}, N_{yy} and N_{xy} moments M_{xx}, M_{yy} and M_{xy} following up on an overlay are gotten by coordination of the stress in each layer or lamina through the cover thickness. Knowing the stress as far as the uprooting, it can get thein-plane force resultant resultants N_{xx}, N_{yy},N_{xy}, M_{xx}, M_{yy} and M_{xy}. The in-plane force resultants are defined as

$$\begin{Bmatrix}\mathrm{N_{xx}}\\ \mathrm{N_{yy}}\\ \mathrm{N_{xy}}\end{Bmatrix} = \int_{-\mathrm{h}/2}^{\mathrm{h}/2} \begin{Bmatrix}\sigma_{xx}\\ \sigma_{yy}\\ \sigma_{xy}\end{Bmatrix}_{\mathrm{k}} \mathrm{dz} = \sum_{\mathrm{k}=1}^{\mathrm{N}} \int_{z_k}^{z_{k+1}} \begin{Bmatrix}\sigma_{xx}\\ \sigma_{yy}\\ \sigma_{xy}\end{Bmatrix}_{\mathrm{k}} \mathrm{dz} \quad (4a)$$

Where σ_x , σ_y and σ_{xy} are normal and shear stress

$$\begin{Bmatrix}N_{xx}\\ N_{yy}\\ N_{xy}\end{Bmatrix} = \begin{bmatrix}A_{11} & A_{12} & A_{16}\\ A_{12} & A_{22} & A_{26}\\ A_{16} & A_{26} & A_{66}\end{bmatrix} \begin{Bmatrix}\varepsilon^0_{xy}\\ \varepsilon^0_{xy}\\ \gamma^0_{xy}\end{Bmatrix} + \begin{bmatrix}B_{11} & B_{12} & B_{16}\\ B_{12} & B_{22} & B_{26}\\ B_{16} & B_{26} & B_{66}\end{bmatrix} \begin{Bmatrix}\varepsilon^1_{xx}\\ \varepsilon^1_{yy}\\ \gamma^1_{xy}\end{Bmatrix} \quad (4b)$$

$$\begin{Bmatrix}M_{xx}\\ M_{yy}\\ M_{xy}\end{Bmatrix} = \int_{-h/2}^{h/2} \begin{Bmatrix}\sigma_{xx}\\ \sigma_{yy}\\ \sigma_{xy}\end{Bmatrix}_k z\, dz = \sum_{k=1}^{N} \int_{z_k}^{z_{k+1}} \begin{Bmatrix}\sigma_{xx}\\ \sigma_{yy}\\ \sigma_{xy}\end{Bmatrix}_k z\, dz \quad (5a)$$

$$\begin{Bmatrix}M_{xx}\\ M_{yy}\\ M_{xy}\end{Bmatrix} = \begin{bmatrix}B_{11} & B_{12} & B_{16}\\ B_{12} & B_{22} & B_{26}\\ B_{16} & B_{26} & B_{66}\end{bmatrix} \begin{Bmatrix}\varepsilon^0_{xy}\\ \varepsilon^0_{xy}\\ \gamma^0_{xy}\end{Bmatrix} + \begin{bmatrix}D_{11} & D_{12} & D_{16}\\ D_{12} & D_{22} & D_{26}\\ D_{16} & D_{26} & D_{66}\end{bmatrix} \begin{Bmatrix}\varepsilon^1_{xx}\\ \varepsilon^1_{yy}\\ \gamma^1_{xy}\end{Bmatrix} \quad (5b)$$

Here, A_{ij} are the extensional stiffness, B_{ij} the coupling stiffness, and D_{ij} the bending stiffness **[12]**.

$$A_{ij} = \sum_{k=1}^{N} (\bar{Q}_{ij})_k \, (z_{k+1} - z_k) \quad (6a)$$

$$B_{ij} = \frac{1}{2} \sum_{k=1}^{N} (\bar{Q}_{ij})_k \, (z^2{}_{k+1} - z^2{}_k) \quad (6b)$$

$$D_{ij} = \frac{1}{3} \sum_{k=1}^{N} (\bar{Q}_{ij})_k \, (z^3{}_{k+1} - z^3{}_k) \quad (6c)$$

3. Experimental Part

3.1 How to manufacture composite material laminated plate mold

To manufacture the mold of composite materials mold, the main steps are summarized in the following:

1-Firstly, cutting the wood mold dimensions (60cm*50cm*10cm).

2-We design the wood and put white specks as constant lines and put spaces between the white spots around 1cm between each point in measurements (30cm*25cm*0.6cm) rectangular shape.

3-Fix at each white guide one nails toward turn into the white point like crisscross at that point put wax on photograph sheet to keep the bond of polyester.

4-Wrap the strands around the nail and we do likewise at each point in longitudinal direct in (90°)for first layer of glass or carbon or hybrid glass with carbon fibers, at that point rehash a similar procedure transverse way in edge (0°) for second layer, and rehash twist filaments longitudinal way in (90°) in third layer to getting on three layers, then we settle the fiber at last with sticky tape, as shown in **figure (2)**.

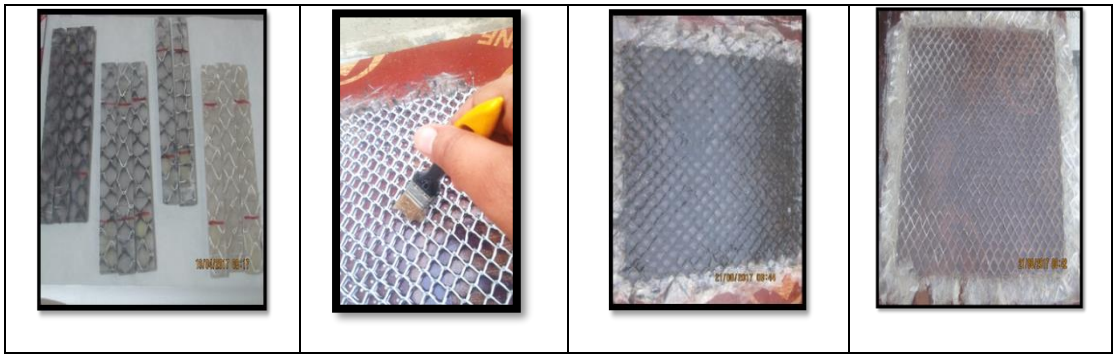

Fig.2: Zig-zag composite materials manufacturing.

5-Place the weight over the cover to guarantee air pockets will move out and the overlay will take smooth surface shape.

6- The overlay will have left for one day at room temperature, and afterward will separated from wood form subsequent to expelling the cover.

7- We use microscope test to watching if the there's any bubbles in composite material.

8- Measurements the overlay by (CNC) machine or by revolving shaper to acquire smooth surface with edges and decreased the thickness to (6mm). Slicing composite materials plate to rectangular examples has measurements (19mm*165mm) utilizing as a part of elastic test.

3.2 Volume fraction

The volume fraction for three types of zig-zag composite materials was investigated experimentally with applying the following relationship:**[11]**

$$V_f = \frac{1}{1+\frac{1-v}{v}\left(\frac{\rho f}{\rho m}\right)} \quad (7)$$

And, the masses ratio is:

$$v = \frac{mf}{mc} \quad (8)$$

Where:

V_f is the volume fraction.

ρ_f , and ρ_m are the densities of fiber and matrix, respectively.

m_f , m_c are the masses of fiber and composite, respectively are calculate by digital weight as shown in **figure (3)**.

Fig. 3: Fibers weighting by a digital weight.

3.3 Mechanical properties of composite materials components:

The tensile experimental test of zig-zag composite materials specimens includes the evaluation of the modulus of elasticity, Poisson's ratio, ultimate tensile strength, yield stress, and Young's modulus of composite materials for three types GFRP, CFRP, and HFRP.

Five samples are used for each test. Every sample is divided according to the dimensions according to ASTM D3039, as shown in **figure (4)**. The device is calibrated by the Central Organization for Standardization and Quality Control.

Fig. 4: Tensile test machine.

Then we stick two strain gauges on a specimen of composite material put one of strain gauges in the place in specimen which expect to happen fracture in tensile test in longitudinal direction to extract and transverse directions then pin it on the sample. We connect the ends of the strain meter to the ends of strain gage and measure the amount of strain in longitudinal direction (ϵ_y) and transverse direction (ϵ_x). See **figure (5)**.

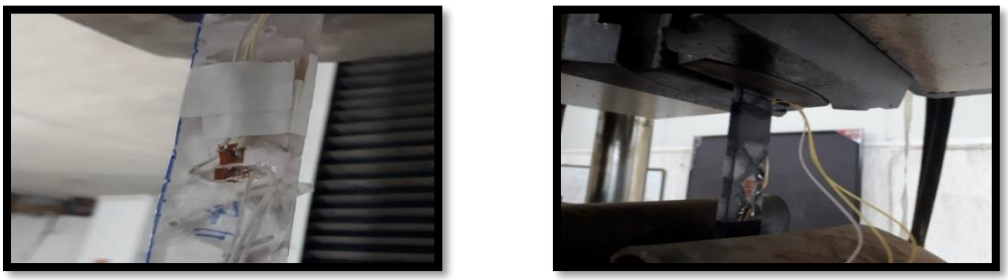

Fig. 5: Poisson's ratio measuring by strain gauges.

3.4 Physical properties

The densities of GFRP, CFRP, and HFRP composite materials are calculated by the following tools:

1. Dial phials, as shown in **figure (6a)**.

2. Sensitive Libras, as shown in **figure (6b)**.

a. Dial Phial **b. Libra sensitive**

Fig. 6: Tools used in experiments to estimate of density.

To complete the tests on piece density for three types of zig-zag composite materials was investigated in density tester as shown in **figure (7)**. The apparatus includes close chamber, hanging which used to overhang the piece of composite materials in the liquid that select according to the type of materials, the container which fills with the amount of liquid. However, the process of test has been

achieved by putting sample into the close chamber and measure the mass of in the air. In addition, the piece immersed into the liquid by an overhang and measures the mass in the liquid. To calculate the density according to the role of Archimedes that refer to the mass in the air per the different of masses (air and liquid) multiply by density of that liquid.

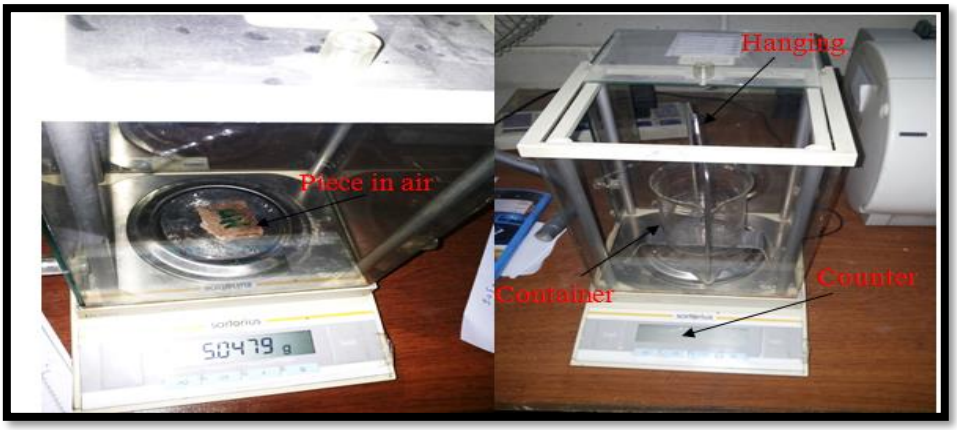

Fig. 7: Density tester.

3.5 Shear stress test

The shear test for three types of composite materials (GFRP, CFRP, and HFRP) is to measure the separation of the layers in the beginning with a sheet of 18 mm thickness. After that, the samples are reduced in the form of a solid. Then process the speciemen to form a (10 mm) solid shaft with a length of 10 cm. See **figure (8)**.

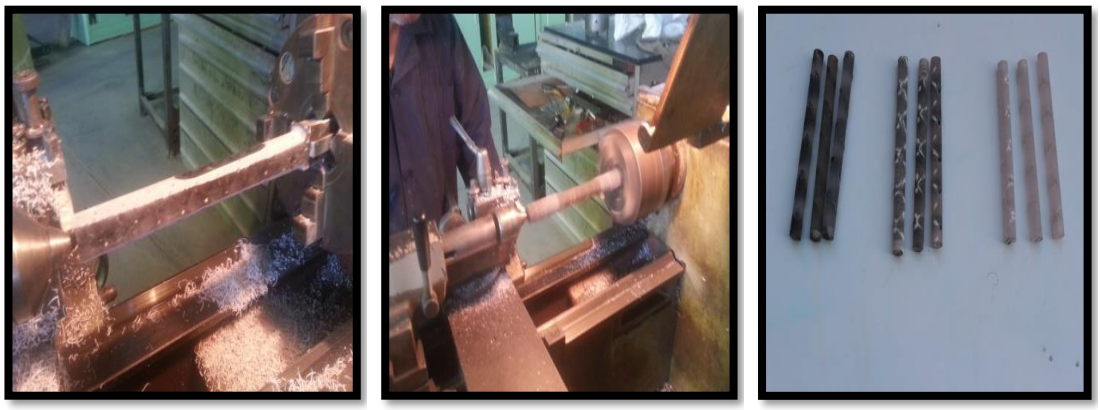

Fig. 8: Shear test samples manufacturing.

The shear stress test procedures is in the following steps:

1. Select proper example, i.e. fragile or bendable metals, composite materials or different materials
2. Measure the transverse measurement with the assistance of a Vernier caliper. For every example, measure no less than three times near the cross segments that are going to be sheared and take their normal esteems.
3. Make the all-inclusive testing machine and shear test apparatus prepared.
4. Determine the most extreme load and load increases from a definitive quality and measurement of the picked example and set up the related programming in understanding.
5. Mount the example in the test installation.
6. Start the loading procedure and carefully watch the harm status of the example until the point that it totally shears.

7. Translate the test connection and apparatus to a safe position and remove the sample. Analyze the uncommon for bending deformation, assuming any.

8. Repeat the try different things with extra samples if important or reestablish the test device and field to finish the test**.** See **figure (9)**.

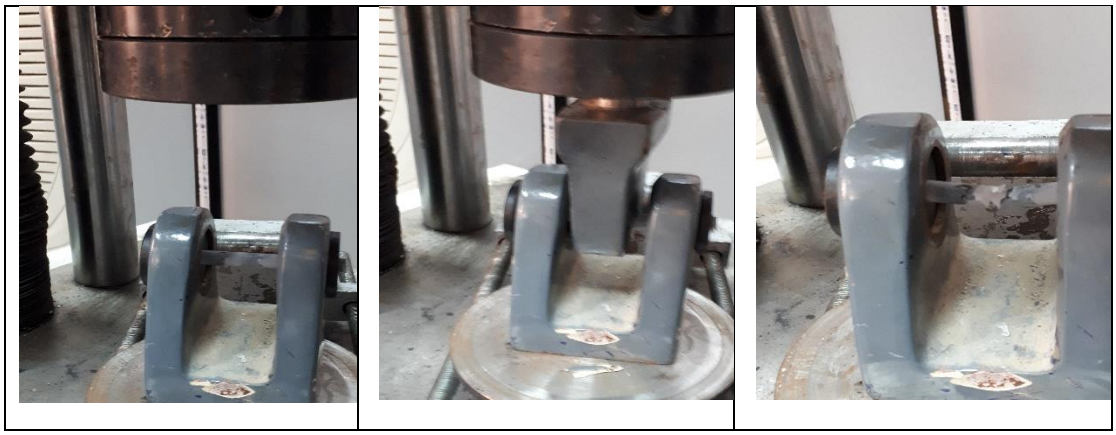

Fig. 9:Shear test device.

3.6 Buckling test

3.6.1 Buckling test with dial gauge

The buckling stress test device is available in Ministry of Sciences and Technology / Materials Department. The buckling stress test procedures is in the following steps:

1.The laminate plates for three types of composite materials (GFRP, CFRP, and HFRP) was loaded statically by uniformly distributed load in longitudinal compression (vertical direction) utilizing tensile test machine of (100kN) capability as shown in **figure (10)**, preparing laminated plates for buckling test has dimensions with constants thickness and width with 6mm and 80 mm, respectively with different lengths (80,160, 240 and 320) mm, after cutting by CNC machine for three types of zig-zag model composite materials.

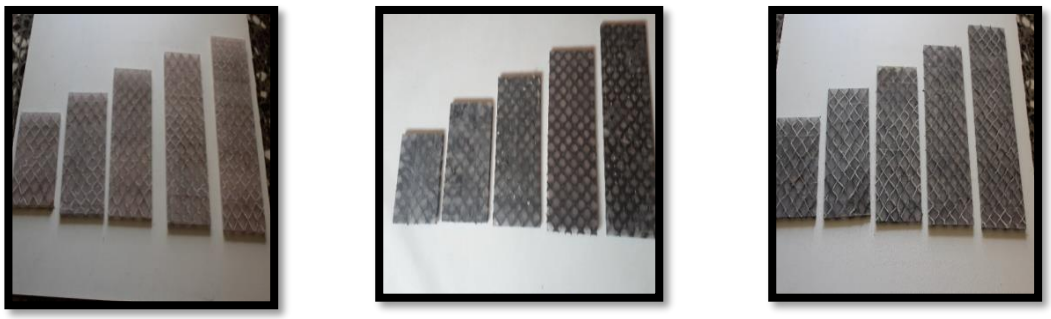

GFRP samples **CFRP samples** **HFRP samples**

Fig. 10: Buckling test samples.

2. The laminate plate is clamped-clamped at two ends and free-free at the other two ends. The specimen was loaded slowly until buckling at room temperature. Clamped-clamped boundary conditions were reenacted along the best and base edges.

3. For axial loading, the test sample was set between two to a great degree solid machine head of which the lower one was settled amid the test, though the upper head was moved downwards by servo water driven chamber. The laminated plate was loaded at steady crosshead speed of (0.5mm/min). **[10]**

4. Put digital dial gauge to measure the deflection during buckling operation through compression test until the specimen has been failure.

We experiment with three types of composite materials firstly; the experimental set up for example GFRP, as shown in **figure (11)**.

Fig. 11: Buckling test for GFRP zig-zag laminate plates by using dial gauges.

5. The buckling load is specified from the load- displacement curve. The vertical displacement has been plotted on the x-axis and load was plotted on the y-axis. For the determination of buckling load as shown in **figure (12)**, the point where left of the straight line is resolved on the designs and the estimation of this point on the y-axis is called as the buckling load. **[13]**

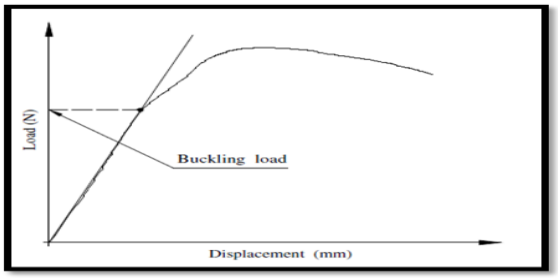

Fig. 12: Load- displacement curve. [13]

3.6.2 Calibration buckling test with dial and strain gauges

The different way for determination buckling load and deflection of buckling by using strain gauges and to check and calibrated the results from the previous method by compression test. Stick three strain gauges on sample type CFRP for example, paste one of strain gages on the sample in the top of the sample, either the second put it in the middle of the sample, the third put it in the middle of the other side. the strain gages connected by wire to device.The first is to examine applied load of the device, either the third sample, measuring the deformation obtained from the extension of the sample, i.e., tensile tension, while the third strain examines the compression resulting from deformation.The strain gauges has measured the deformation in the form of tensile it is the deflection of buckling load. See **figure (13)**.

Fig. 13: Buckling load and deflection for CFRP composite laminated plates measuring by using strain gauges.

To calibrate the results obtain by compression test and the results from strain gauges utilizing device strain meter and using dial gage put the sensor of dial gage on specimen, then operating compression test. See **figure (14)**. While the strain gauges read the signals was sent from strain gauges to show on the screen of a computer looks like three waves (white, red and green) for each one of strain , in the same time dial gauge is reading the deflection in the plate.

Fig. 14: Calibration between measuring deflection by dial gauge with strain gauge.

4. Numerical Part

For the purpose of the present work. ANSYS software program was used to simulate thean element called shell 181 is selected which is suitable for analyzing thin to moderately thick shell structures, it is suitable for analyzing thin to moderately thick shell structures. **[14]**

It is a four-node element with six degrees of freedom at each node: translations in the x, y, and z directions, and rotations about the x, y, and z-axes. (If the membrane option is used, the element has translational degrees of freedom only), Pressure may be input as surface loads on the element faces as shown by the circled numbers in **figure (15)**.

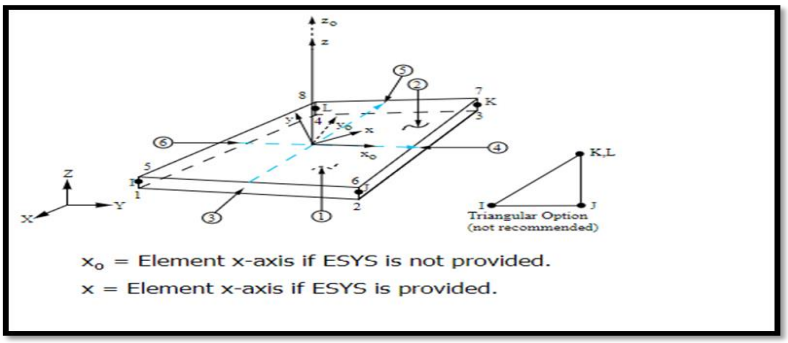

Fig .15: Shell 181 stress output. [14]

5. Results and Discussion

The present work focused mainly on the buckling behavior of three types of GFRP, CFRP, and HFRP clamped-clamped composite materials rectangular laminate plates for a zig-zag model subjected to static uniformly distributed load under room temperature. This section contains the experimental and numerical results with discussion as shown in the following steps:

5.1 Experimental results

In the present work, the experimental results and discussion are divided to:

5.1.1Physical results

5.1.1.1 Dimensions results

The average thicknesses, cross sectional areas for three types of zig-zag composite materials laminate plates (GFRP, CFRP, and HFRP), are measured by using a digital sensitive weighting device. These dimensions are tabulated in **table (1)**.the lengths is variable with fixed width and thickness.

Table 1: Composite laminated plates dimensions for zig-zag model.

Composite materials type	No. of layers	Thickness * width * length (mm^3)	Cross-sectional area (mm^2)
GFRP	8	6.2*80* variable	496
CFRP	8	6.4*80*variable	512
HFRP	8	6.1*80*variable	488

5.1.1.2 Volume fractions results

The volume fraction results have been found from mathematical operation. The low volume fraction for the three types of composite materials because of the lowness of weight of fibers and the fiber-bonding mode in the form of zig-zag creates large and large blanks inside the sample filled with polyester which makes it larger and heavier than fiber.

When binding around the nails will cause an increase in the thickness of the sample, which leads to the lack of control of the thickness of the plate, which makes the plate is heterogeneous and need to be softened and reduce the thickness. The volume fractions for three types of zig-zag composite materials are listed in **table (2)**.

Table 2: Volume fraction experimental results.

Composite materials type	Volume fraction (%)
GFRP	13.08
CFRP	12.01
HFRP	12.77

5.1.1.3 Densities results

Density tests for three types of zig-zag composite materials laminate plates (GFRP, CFRP, and HFRP), can be achieved by using Archimedes role which depended on masses in the air and in the water.

The results was observed that the densities obtained from other sources {theoretically by using the equation $\boldsymbol{\rho = \frac{m}{V}}$ and experimentally, the pure materials densities results obtained from the practical experience are very close and the error rate is acceptable within the limits. The maximum percentage error is 6.8%. See **table (3)**.

Table 3: Pure materials densities experimental results.

Pure material	Theoretical density (g/mm^3)	Experimental density (g/mm^3)	Error (%)
E-glass fiber (ρ_g)	2.540	2.367	6.81
Carbon fiber (ρ_c)	1.820	1.744	4.17
Polyester (ρ_m)	1.130	1.106	2.12

Table (4) shows the three types of zig-zag composite materials densities results. The maximum percentage error between theoretical and experimental results is 6.8%.

Table 4: Composite materials densities theoretical and experimental results.

Composite materials type	Theoretical densities (g/mm^3)	Experimental densities (g/mm^3)	Error (%)
GFRP	1.609	1.555	5.40
CFRP	1.519	1.479	4.00
HFRP	1.470	1.402	6.80

5.1.2 Mechanical properties results

Fifteen samples standard flat specimens (three types of zig-zag laminations GFRP, CFRP, and HFRP), were tested by using tensile test under room temperature (23ºC) and characterized by a maximum load (0-100 kN) with feed rate (0.005-200 mm/min). Load-extension curves, for three types of zig-zag composite materials, is using to find the mechanical properties (Young modulus, yield stress, ultimate tensile stress and Poisson's ratio). **Table (5)** shows these results.

Table 5: Mechanical properties experimental results of a zig-zag model.

Composite materials type	Longitudinal modulus of elasticity E_1 (GPa)	Transverse modulus of elasticity E_2 (GPa)	Ultimate tensile stress σ_{ult} (MPa)	Yield stress σ_y(MPa)	Poisson's ratio (v)
GFRP	1.52	1.40	29.40	20.25	0.22
CFRP	2.02	1.90	31.95	22.82	0.27
HFRP	1.44	1.42	29.72	19.17	0.37

Modulus of elasticity for longitudinal direction (E_1) is very closer from transverse of modulus of elasticity (E_2) reaching to identify. Note that the mechanical properties for CFRP is higher than for GFRP and HFRP.

We stick two strain gauges on specimen of composite material put one of strain gauge in the place in specimen, which expect happen fracture in tensile test. Dividing $\epsilon y / \epsilon x$ to find Poisson's ratio results for three types of zig-zag composite materials laminated plates for GFRP, CFRP, and HFRP. These results are listed in table (5).yield stress has found from force-displacement curve.

5.1.3 Shear test results

Table (6) shown the maximum shear stress results under room temperature (23oC) for three types of zig-zag composite materials for GFRP, CFRP, and HFRP. These results show the shear stress value of CFRP is greater than that values of GFRP and HFRP.

Table 6: Maximum shear stress experimental results for three types of zig-zag composite materials.

Composite materials type	Maximum shear stress (MPa)
GFRP	19.653
CFRP	27.915
HFRP	20.190

5.1.4 Buckling test results

5.1.4.1 Critical buckling load results

The results of buckling test under room temperature (23oC) for three types of zig-zag composite materials laminated plates is clamped-clamped from two sides and free-free from other sides, are shown in table (7). The results in this table show the ultimate buckling stress value of CFRP is greater than that values of GFRP and HFRP. The results of experimental critical buckling load for three types of composite materials laminated plates model zig-zag with different aspect ratios (a/b = 1, 2, 3, and 4) and with constant thickness ratios (b/t = 13.333) are shown in table (7). These results shown the critical buckling load is decrease when the aspect ratio is increase under constant thickness ratio, and the critical buckling load values for CFRP rectangular laminate plates is greater than that in GFRP and HFRP at constant the aspect and thickness ratio.

Table 7: Critical buckling load experimental results for different aspect ratio.

Dimensions (length*width)	Critical buckling load of GFRP (kN)	Critical buckling load of CFRP (kN)	Critical buckling load of HFRP (kN)
(80mm*80mm) i.e. (a/b = 1)	9.2	10.4	8.1
(160mm*80mm) i.e. (a/b = 2)	3.2	4.5	3.1
(240mm*80 mm) i.e. (a/b = 3)	1.8	2.5	1.7
(320mm*80mm) i.e. (a/b = 4)	1.1	1.5	1.0

To extract the shear force and compare it with the critical buckling load that mean the delamination is happen or not. If the critial bukling force is less than the shear force, this means that the separation of layers is not occurs and this mean that the manufaturing of composite materials laminated plates is a good. See **table (8)**.

Table 8: Comparison between experimental shear and ultimate buckling stresses resuls.

Composite materials type	Shear stress τ (MPa)	Ultimate buckling stress σ_{buck} (MPa)	Delaminating
GFRP	19.653	18.54	Not happen
CFRP	27.915	20.31	Not happen
HFRP	20.19	16.58	Not happen

5.1.4.2 Maximum deflection under critical buckling load results and discussion by using dial gauge

The laminated plate buckled globally until complete failure occurred. Experimental critical buckling load is taken from load-displacement curve. **Table (9)** shows the maximum deflection results under critical buckling load that measured by dial gauge. These results shown the maximum deflection values is increase when the aspect ratio is increase under constant thickness ratio because of the plate which need more force when the length decrease.

Table 9: Maximum experimental deflection results under critical buckling load

Dimensions (length*width)	Maximum deflection GFRP (mm)	Maximum deflection CFRP (mm)	Maximum deflection HFRP (mm)
(80mm*80mm) i.e. (a/b = 1)	21.5	16.7	17.5
(160mm*80mm) i.e. (a/b = 2)	29.2	25.2	22.8
(240mm*80 mm) i.e. (a/b = 3)	47.8	36.2	33.9
(320mm*80mm) i.e. (a/b = 4)	76	46.4	41.5

From the results of table (9), the maximum deflection values are increase when the aspect ratio is increase under constant thickness ratio, also the maximum deflection in GFRP composite materials rectangular laminated plates is greater than that in CFRP and HFRP.The E-glass have mechanical properties is best from the other types.

5.1.4.3 Utilizing strain and dial gauges matching to measure and calibrate the buckling deflection

We choose CFRP laminated plate results with aspect ratio (a/b = 1) for example, from **tables (5.8)** and **(5.10)** results that obtaining from dial gauge only with the results shows in **table (10)** that obtaining from strain gauge matching with dial gauge test to compare and calibrate these results. **Table (10)** and **figure (17)** shown the graduated buckling deflection with graduated critical buckling load.

Table 10: Critical buckling results for CFRP by using strain and dial gauges

Critical buckling load (kN)	0.5	1	2	4	7	8	9	10.5
Maximum buckling deflection(mm)	0	0	0	1	3	5.5	7.5	16.5

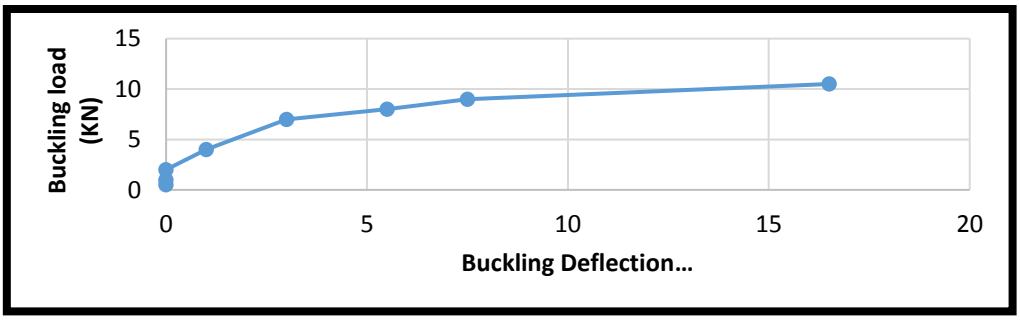

Fig. 17: Buckling load against buckling deflection using strain gage matching with dial gauge for rectangular laminate plate with (a/b = 1) for composite materials type CFRP.

A good agreement is achieved between the two experimental ways for determining the critical buckling load and maximum buckling deflection results, the maximum absolute percentage error rates are about 1% and 1.1%, respectively.

5.2 Numerical Results

5.2.1 Critical buckling load results

Table (11) shows the critical buckling load numerical results versus aspect ratio for three types of composite materials rectangular laminated plates for a zig-zag model, by using finite elements technique (ANSYS program 15.0). Generally, the critical buckling load is decrease when the aspect ratio is increase.

Table 11: Critical buckling load numerical results for different aspect ratio.

Dimensions (length*width)	**Critical buckling load GFRP (kN)**	**Critical buckling load CFRP (kN)**	**Critical buckling load HFRP (kN)**
(80mm*80mm) i.e. (a/b = 1)	13.03	14.90	15.23
(160mm*80mm) i.e. (a/b = 2)	4.82	7.35	6.58
(240mm*80 mm) i.e. (a/b = 3)	2.78	3.22	3.61
(320mm*80mm) i.e. (a/b = 4)	1.46	2.74	2.22

5.2.2 Maximum buckling deflection results

The dimensions of the three types of composite materials laminated plates for a zig-zag model were used in this work are mentioned in **figures (18), (19),** and **(20)** with **table (12)** as shown below, with critical buckling load numerically results by using ANSYS program15.0.

Generally, from numerical results are shown in these figures and table above, the maximum deflection is increase when the aspect ratio is increase under constant thickness ratio. The values of maximum deflection at critical buckling load in GFRP composite rectangular laminate plates for a zig-zag model are greater than these values in CFRP and HFRP, because of the GFRP plates is more ductility than in CFRP and HFRP plates.

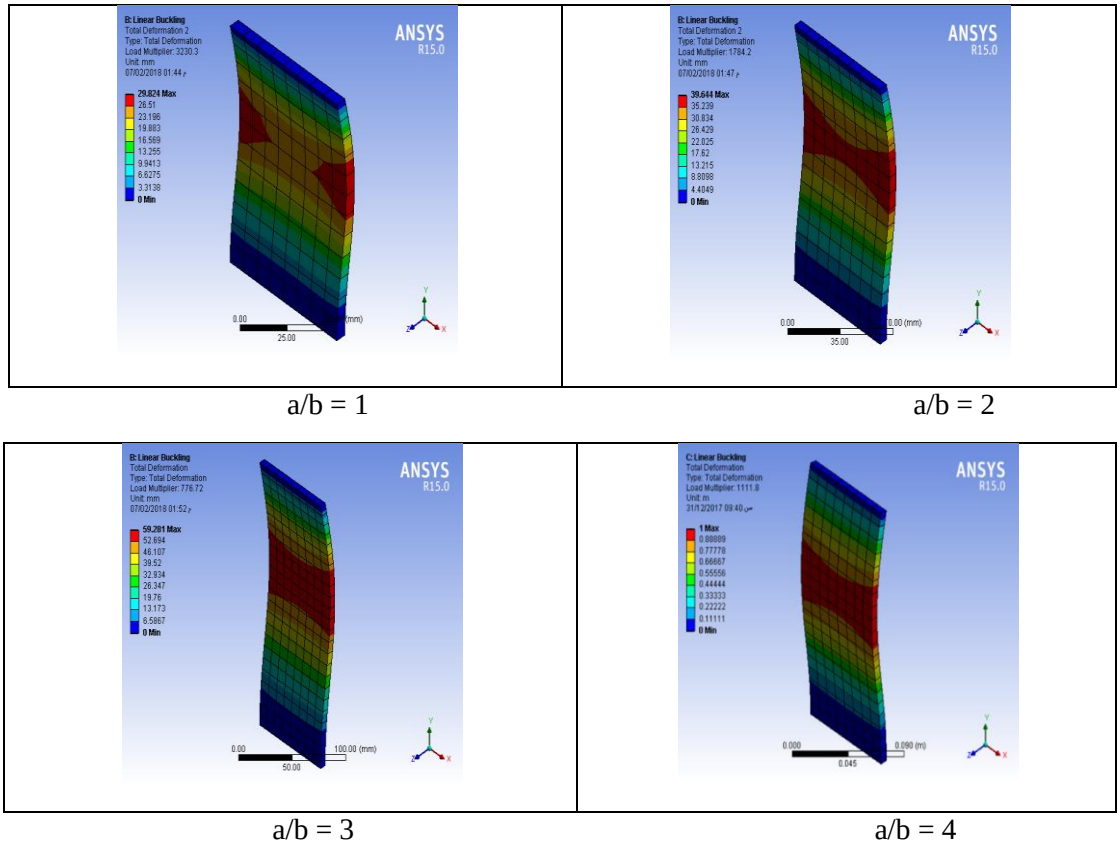

Fig.18: Numerical deflection maps for zig-zag GFRP composite materials rectangular laminated plates with different aspect ratios.

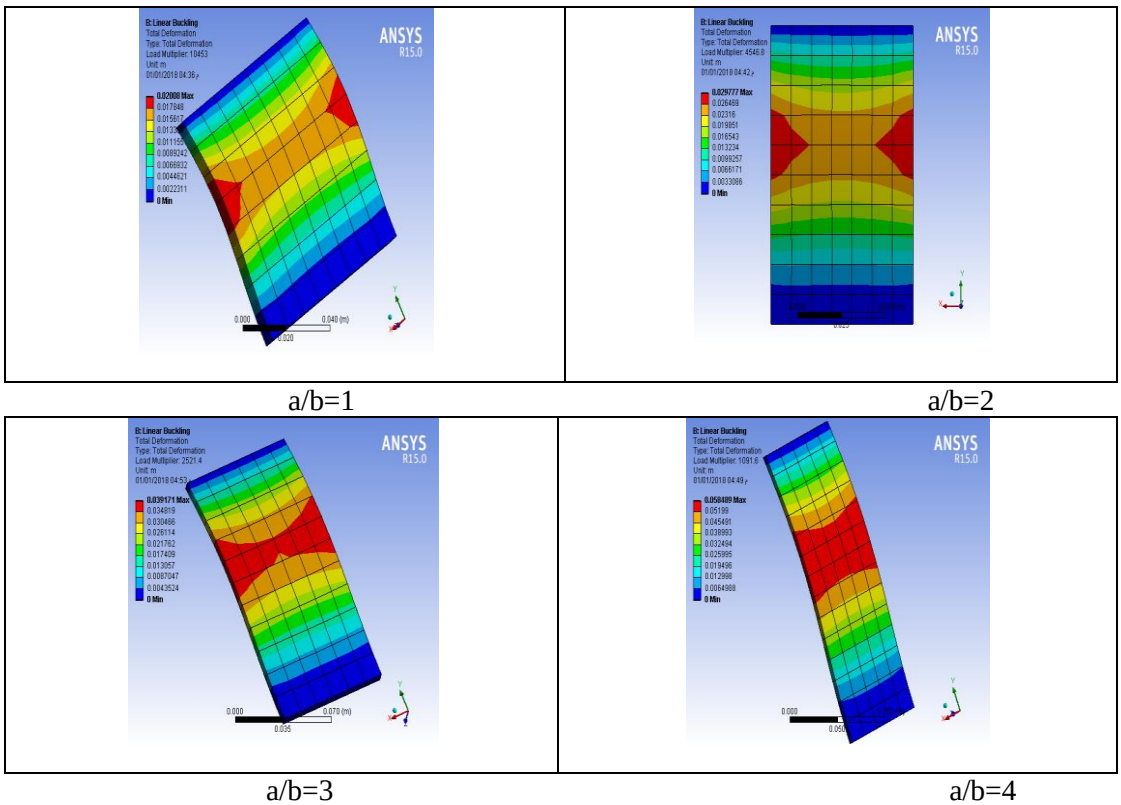

Fig. 19: Numerical deflection maps for zig-zag CFRP composite materials rectangular laminated plates with different aspect ratios.

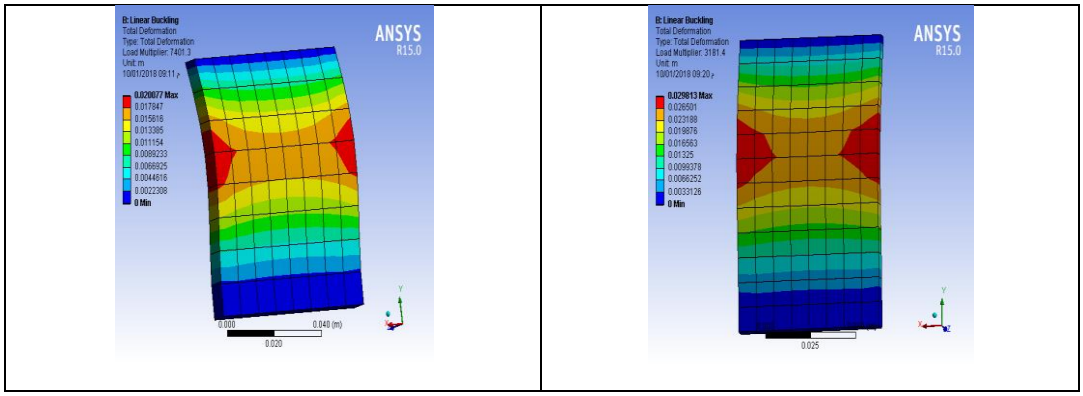

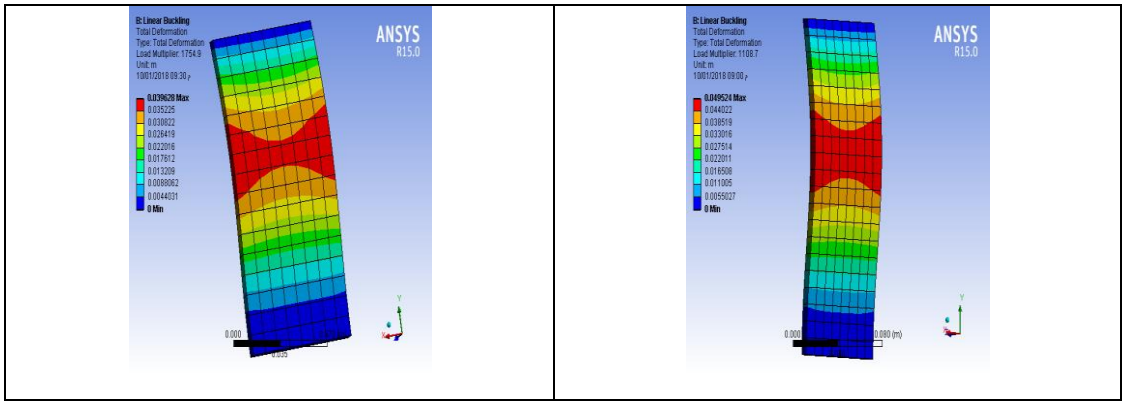

Fig. 20: Numerical deflection maps for zig-zag HFRP composite materials rectangular laminated plates with different aspect ratios.

Table 12: Maximum deflection numerical results under critical buckling load for three types of composite laminated plates.

Dimensions (length*width)	Maximum deflection GFRP (mm)	Maximum deflection CFRP (mm)	Maximum deflection HFRP (mm)
(80mm*80mm) i.e. (a/b = 1)	29.28	20.08	20.07
(160mm*80mm) i.e. (a/b = 2)	39.64	29.77	29.81
(240mm*80 mm) i.e. (a/b = 3)	50.28	39.17	39.62
(320mm*80mm) i.e. (a/b = 4)	100.00	58.18	49.52

5.3 Comparison between Numerical and Experimental Results

5.3.1 Critical buckling load versus aspect ratio results

Generally, because either there may be bubbles or porosity in a part of specimen or its thickness is not uniform exactly or the fibers are not straight in a part or thickness of each layer is not constant the critical buckling load is decreasing when aspect ratio is increasing. It was obvious that the experimental buckling load value is less than the numerical value in all cases. **Figures (21)**, **(22)**, and **(23)** shows comparison between the experimental and numerical results for three types of zig-zag GFRP, CFRP, and HFRP composite materials of clamped – clamped rectangular laminated plates, respectively.

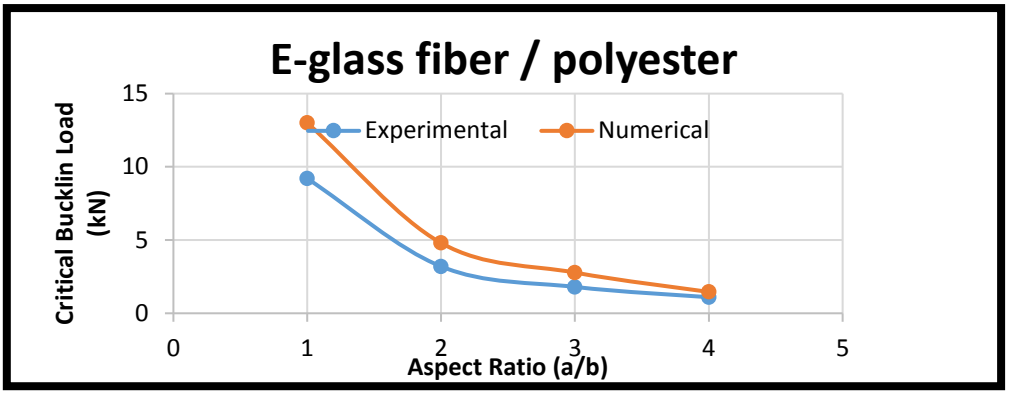

Fig. 21: Critical buckling load against aspect ratio for zig-zig GFRP composite materials of clamped – clamped rectangular laminated plate.

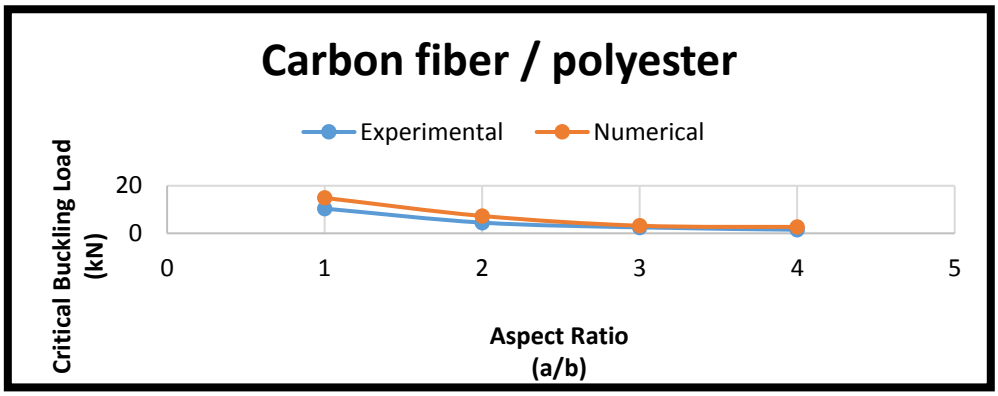

Fig. 22: Critical buckling load against aspect ratio for zig-zig CFRP composite materials of clamped – clamped rectangular laminated plate.

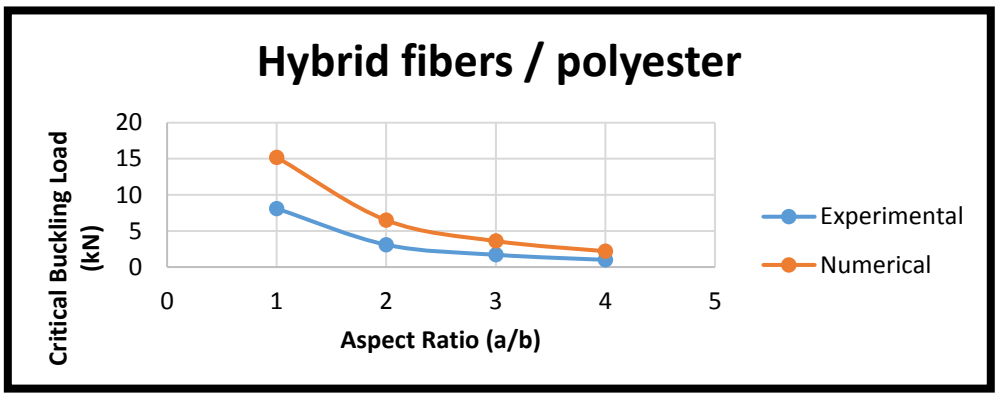

Fig. 23: Critical buckling load against aspect ratio for zig-zig HFRP composite materials of clamped – clamped rectangular laminated plate.

From these figures shows the maximum percentage errors between the experimental and numerical results are 29.23%, 30.20%, and 46.71% at aspect ratio (a/b = 1) for GFRP, CFRP, and HFRP, respectively.

5.3.2 Critical buckling load versus maximum deflection results

The critical buckling load is decrease when the maximum deflection is increases.

It was obvious that the experimental buckling load value is less than the numerical value in all cases because. Figures **(24)**, **(25)**, and **(26)** shows comparison between the experimental and numerical results for three types of zig-zag GFRP, CFRP, and HFRP composite materials of clamped – clamped rectangular laminated plates, respectively.

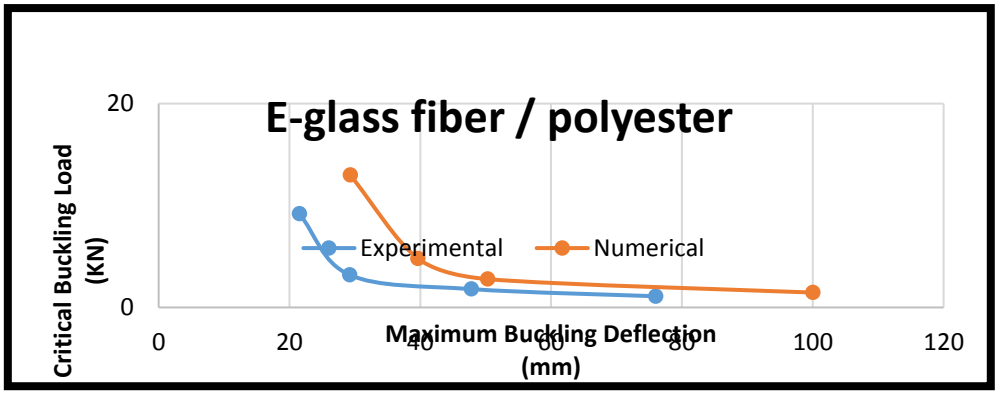

Fig. 24: Critical buckling load against maximum deflection for zig-zig GFRP composite materials of clamped – clamped rectangular laminated plate.

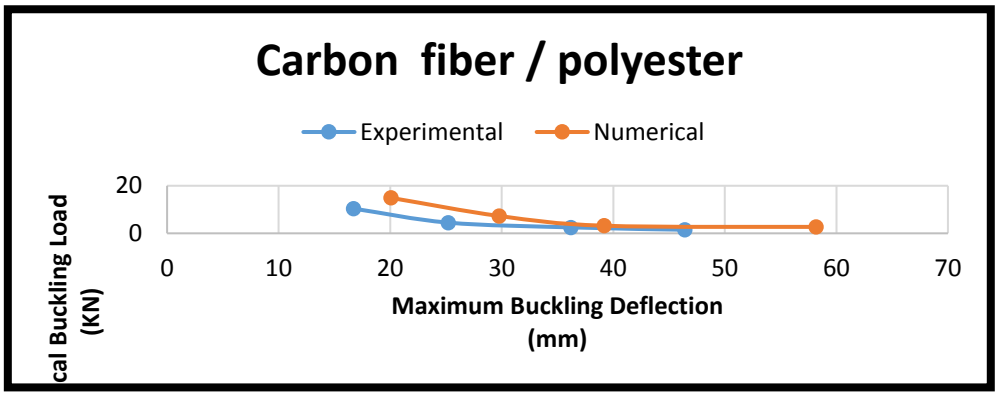

Fig. 25: Critical buckling load against maximum deflection for zig-zig CFRP composite materials of clamped – clamped rectangular laminated plate.

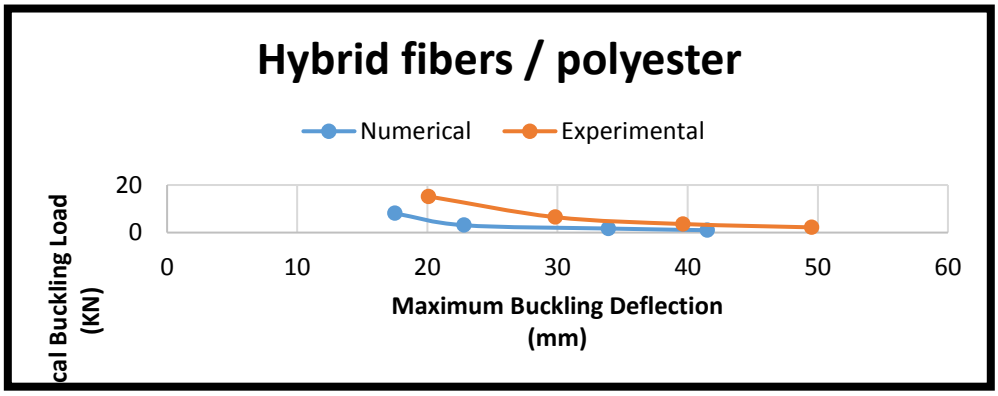

Fig. 26: Critical buckling load against maximum deflection for zig-zig HFRP composite materials of clamped – clamped rectangular laminated plate.

6. Conclusions

The buckling phenomenon in thin plates under different loading is fundamental in many engineering domains for their structural safeness appreciation. In the current work, the buckling behavior of critical buckling load for thin laminated plate of three types of composite materials (GFRP, CFRP, and HFRP) for a zig-zag model has been studied experimentally and numerically.

From the previous discussion of the results the following conclusions can be drawn out from the present study:

1.The mechanical properties of the laminated plates found for zig-zag fibers has improved compared to its counterparts of composite orthogonal ($0^o/90^o$) fibers type composite laminate plates, the percentage improving are (20.3% of yield stress, 29.7% of ultimate tensile stress, 14.7% of

longitudinal Young's modulus and 10.9% of transverse Young's modulus) for GFRP, (12.6% of yield stress, 15.8% of ultimate tensile stress, 10.5% of longitudinal Young's modulus and 16.9% of transverse Young's modulus)for CFRP, and (7.6% of yield stress, 9.8% of ultimate tensile stress, 13.3% of longitudinal Young's modulus and 11.9% of transverse Young's modulus)for HFRP.

2.The mechanical properties of CFRP composite materials for a zig-zag model are higher than that for GFRP and HFRP.

3.From three types of zig-zag composite materials densities results, the maximum percentage error between theoretical and experimental results is 6.8%.

4.The shear stress for CFRP is larger than GFRP and HFRP. So, that the delaminating in CFRP is not happen, which is far from the delaminating and then come after the fibers of HFRP followed GFRP.

5.The critical buckling load is decrease when the aspect ratio is increase under constant thickness ratio, and the critical buckling load values for CFRP rectangular laminate plates is greater than that in GFRP and HFRP at constant the aspect and thickness ratio.

6.The maximum deflection value is increase when the aspect ratio is increase under constant thickness ratio, also the maximum deflection in GFRP composite materials rectangular laminated plates is greater than that in CFRP and HFRP.

7. A good agreement is achieved between the two experimental ways for determining the critical buckling load and maximum buckling deflection results, the maximum absolute percentage error rates are about 1% and 1.1%, respectively.

8. The maximum percentage difference between the experimental and numerical results are 29.23%, 30.20%, and 46.71% at aspect ratio (a/b = 1) for GFRP, CFRP, and HFRP, respectively. This is due to several reasons, including the improper manufacturing process and the presence of bubbles during the casting process.

References

[1] Lee K. H., Lin W. Z., and Chow S. T.," Bidirectional Bending of Laminated Composite Plates Using an Improved Zig-Zag Model", Composite Structures 28, pp 283-294, Elsevier Science Limited,1994.

[2] Austin, C. D.," Buckling of Symmetric Laminated Fiber-Glass Reinforced Plastic (FRP) Plates", M.Sc. thesis, University of Pittsburgh, 2003.

[3] Esfahani M. N., Nejad H. G., and Barington P. E.,"Experimental and Numerical Buckling Analysis of Delaminated Hybrid Composite Beam Structures", Applied Mechanics and Materials Vols. 24-25, pp 393-400, 2010.

[4] Ahmed N.H., Numerical and Experimental Investigation Mechanical and Thermal Buckling Loads of Laminate Composite Materials M.Sc. thesis, College of Engineering, Baghdad University, 2011.

[5] Gaira N. S., Maurya N. K. and Yadav R. K., "Linear Buckling Analysis of Laminated Composite Plate", International Journal of Engineering Science & Advanced Technology Vol.2, Issue 4, pp886 – 891., 2012.

[6] Al Humdany A., Theoretical and Numerical Analysis for Buckling of Antisymmetric Simply Supported Laminated Plates under Uniaxial Loads, Journal of Karbala University, Vol. 10 No.4 Scientific, 2012.

[7] Joshi A., Ravinder Reddy P., Krishnareddy V. N., and SushmaCh.," Buckling Analysis of Composite Materials for Thin Carbon / Epoxy Plate with Circular Cut-Outs under Biaxial Compression by Using FEA", International Journal of Research in Engineering and Technology,Vol. 02 Issue. 10., 2013.

[8] Ealavarasan T., Selvarasu S., Experimental Investigation and Buckling Analysis of Woven Glass Epoxy Laminated Composite Plate, International Journal of Innovative Research in Science Engineering and Technology, Vol. 4, Special Issue 6, May 2015.

[9] Rajappan, Magesh, and Gurunathan," Buckling Analysis in Unidirectional Glass Epoxy Laminated Plate", International Conference on Recent Advancement in Mechanical Engineering & Technology, Vol. 4, Issue. 5, 2015.

[10]Kubiak T.,"Dynamic Buckling of Thin-Walled Composite Plates with Varying Widthwise Material Properties", Int J Solid Struct 45: pp.5555–5567, 2005.

[11]Reddy J.N.," Mechanics of Laminated Composite Plates and Shells: Theory and Analysis". 2ed; CRC Press, 2004.

[12] "Theory, Analysis, and Element Manuals", ANSYS 11 Program.

[13]Cho M., and Kim J.S, Higher-Order Zig-Zag Theory for Laminated Composites with Multiple Delaminations, AIAA J., 37 p.p. 774-777 .19, 2001.

[14] ANSYS 2012, ANSYS Mechanical APDL Structural Analysis Guide, ANSYS, Inc., U.S.A.2001; 14:406-11.

[15] Madenci E. and Guven I. ,"The Finite Element Method and Applications in Engineering using ANSYS", New York: Springer, 2006.

[16] Mosheer.A.K., "Effect of Variable Fiber Spacing on Buckling Strength of Composite Plates" Journal of Babylon University/Engineering Sciences/ No.(2)/ Vol.(22),pp 526., 2014.

سلوك الانبعاج لمواد مركبة رقيقة مستطيلة المثبتة الاطراف لنموذج متعرج الطراز

حسام حسين علي **مجيد حبيب فيض الله**

قسم الهندسة الميكانيكية، كلية الهندسة، جامعة بغداد، بغداد، العراق

E-mail: dr_majidhabeeb@yahoo.com E-mail: ha391799@gmail.com

الخلاصة

هذا البحث ركز بصورة رئيسية على سلوك الانبعاج للصفائح المستطيلة الرقيقة متعرجة الطراز مصنعة من ثلاثة أنواع من المواد المركبة وهي (ألياف الزجاج / البوليستر، ألياف الكاربون / البوليستر وألياف هجينة من ألياف الزجاج والكاربون معا / البوليستر) والمسلطة عليها أحمال انبعاج ستاتيكية ويجرى الاختبار عند درجة حرارة الغرفة. وقد تم دراسة تأثير نوع واحد من الشروط الحدية حيث تم تثبيت الصفائح من جهتين وحررت من الجهتين الأخرى. تحليل الانبعاج لهذه الصفائح درست عددياً وعمليا مع اختلاف نسبة الأطوال وثبوت نسبة السمك. الجانب العملي تضمن تصنيع صفائح رقيقة مصنعة من (ألياف الزجاج / البوليستر، ألياف الكاربون / البوليستر وألياف هجينة من ألياف الزجاج والكاربون معا / البوليستر) متعرجة الطراز، ثم استخراج الخصائص الميكانيكية لها عن طريق اختبار الشد والتي هي (معامل المرونة، إجهاد الخضوع، أعظم مقاومة شد، ونسبة بويسون).

تضمن الجانب العملي كذلك اختبار القص لنماذج ثلاثة أنواع من المواد المركبة لمعرفة إمكانية حدوث الانفصال الطبقي أم لا أثناء اختبار الانبعاج.

كما وان الجانب العملي استخدم لإيجاد حمل الانبعاج الحرج وأعظم انحراف للأنواع الثلاثة من الصفائح المستطيلة الطبائقية متعرجة الطراز تحت تأثير نسبة الأطوال وعند حمل ضغط ستاتيكي موزع بانتظام.

تم حساب حمل الانبعاج الحرج وأقصى انحراف من التحليل العددي للأنواع الثلاثة من الصفائح المستطيلة الطبائقية متعرجة الطراز تحت تأثير نسبة الأطوال وعند حمل ضغط ستاتيكي موزع بانتظام، حيث استخدمت طريقة العناصر المحددة من خلال برنامج انسس 15.

الاستنتاج الرئيسي من هذا البحث هو ان استخدام الطراز المتعرج في تصنيع صفائح المواد المركبة قد حسن من الخصائص الميكانيكية لها كما وان حمل الانبعاج الحرج قد ازداد.

إن النتائج العملية والعددية كانت ذات نسب خطأ مئوية مقدارها 29.23%، 30.20%، و46.71% عند نسبة أطوال (a/b) 1 = للأنواع الثلاثة من المواد المركبة وهي (ألياف الزجاج / البوليستر، ألياف الكاربون / البوليستر وألياف هجينة من ألياف الزجاج والكاربون معا / البوليستر) على الترتيب.

ان قيمة الانحراف العظمى الناتجة من الانبعاج تزداد مع زيادة نسبة الأطوال وتحت ثبوت نسبة السمك، كما وان أعظم انحراف في صفائح المواد المركبة من نوع ألياف الزجاج / البوليستر متعرجة الطراز اعلي من نظيراتها المكونة من ألياف الكاربون / البوليستر وألياف هجينة من ألياف الزجاج والكاربون معا / البوليستر.

هنالك تطابق جيد تحقق في نتائج الطريقتان العمليتان للحصول على حمل الانبعاج الحرج وأعظم انحراف ناتج من الانبعاج، وان أعظم نسبة معدل خطأ مطلق كان حوالي 1% و1.1% على الترتيب

الكلمات الداله: – تحليل الانبعاج، مواد مركبة النوع المتعرج، صفائح مثبتة الاطراف، برنامج أنسز R.15